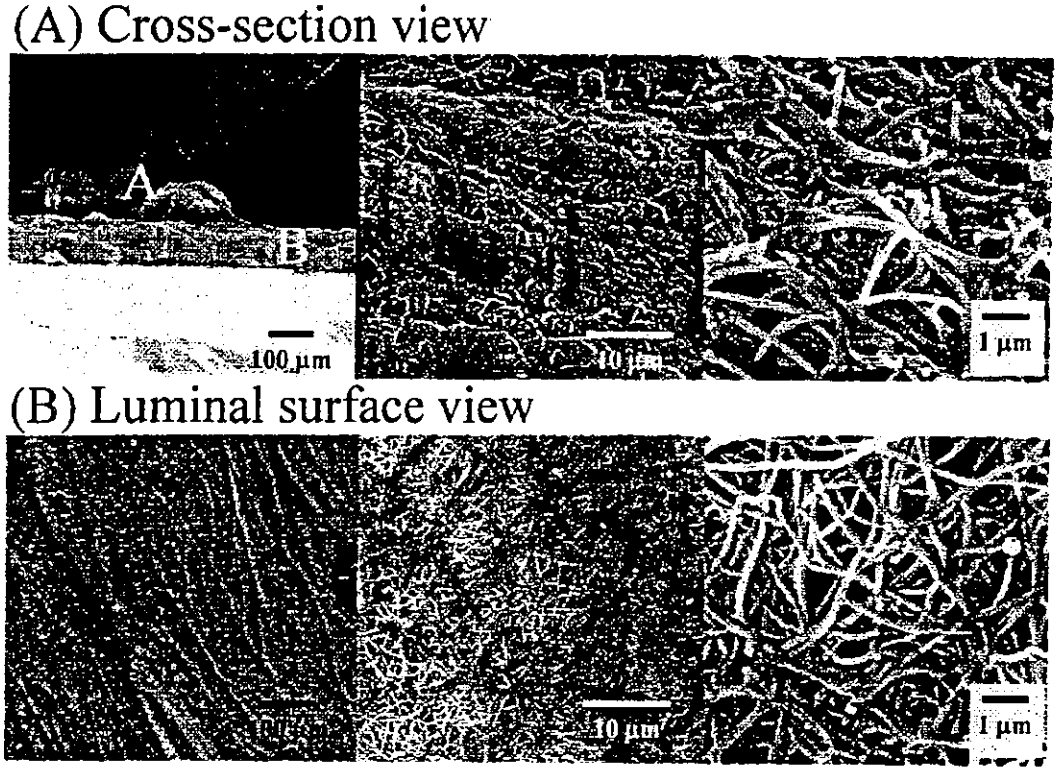

Figure 4. Scanning micrograph of cross-sectional *(A)* and luminal *(B)* views of in situ–formed collagen mesh at different magnifications (magnification is enlarged from left to right). Note that *A* in the cross-sectional view with the lowest magnification denotes the dense collagen meshes formed in micropores when squeezed, and *B* denotes a dense collagen mesh layer.

α-actin (for smooth muscle cells), all of which were purchased from Dakó Corp, were used as primary antibodies, respectively, and the biotin-avidin-peroxidase–labeled rat anti-rabbit IgG served as the secondary antibody to identify the cell types in the neoarterial wall of the grafts.

Results

Mononuclear cells in peripheral blood isolated by means of the centrifugal gradient density technique were cultured in collagen-coated dishes. The majority of isolated mononuclear cells died within 2 to 3 weeks of culture. Colonies of proliferating cells appeared at approximately 10 days, and the primary culture of the surviving cells (n = 6) was continued for 17.3 ± 6.5 days before subculture. The harvest rate of EPCs was approximately 15% (blood volume per sample, 15 mL; total number of samples, 40; number of generations of colony, 12; number of proliferative EPCs, 6). Figure 2 demonstrates that the subcultured cells exhibited a cobblestone-like morphology (Fig 2, *A*), positive uptake of fluorescence-labeled acetylated low-density lipoprotein (Fig 2, *B*), and positive staining of the factor VIII–related antigen (Fig 2, *C*) and Flk-1 (Fig 2, *D*). These cells also produced NO intracellularly, which was proved by means of intracellular staining with an NO-specific indicator, DAF-2DA (Fig 2, *E*). Our experiments showed that approximately 4.2 ± 1.2 × 10^6 EPCs were regularly obtained after 16 ± 4 days at 1 to 2 passages of subcultures. The PDT during the exponential stage of cell proliferation, which started from 2 to 3 days after subculture and was semiquantatively determined, ranged from 23 to 29 hours, and the average PDT calculated was 24.2 ± 2.5 hours (Figure 3).

The hybrid vascular graft, which is composed of a confluent EPC monolayer, dense collagen fiber mesh layer, and microporous thin SPU film, was prepared according to the schematic shown in Figure 1. Briefly, after a collagen gel was formed in the interspace between a mold consisting of an inner glass mandrel and an outer glass sheath, a microporous SPU film was wrapped and squeezed tightly to expel water out to form dense collagenous fiber meshes, as shown in Figure 4. Collagen meshes completely covered the luminal surface of an SPU tube in which micropores were filled with collagen meshes. After tight wrapping with the microporous SPU film and suturing, the glass mandrel was carefully removed to leave a collagen mesh-lined SPU tube. EPCs were seeded on the luminal surface of the graft and

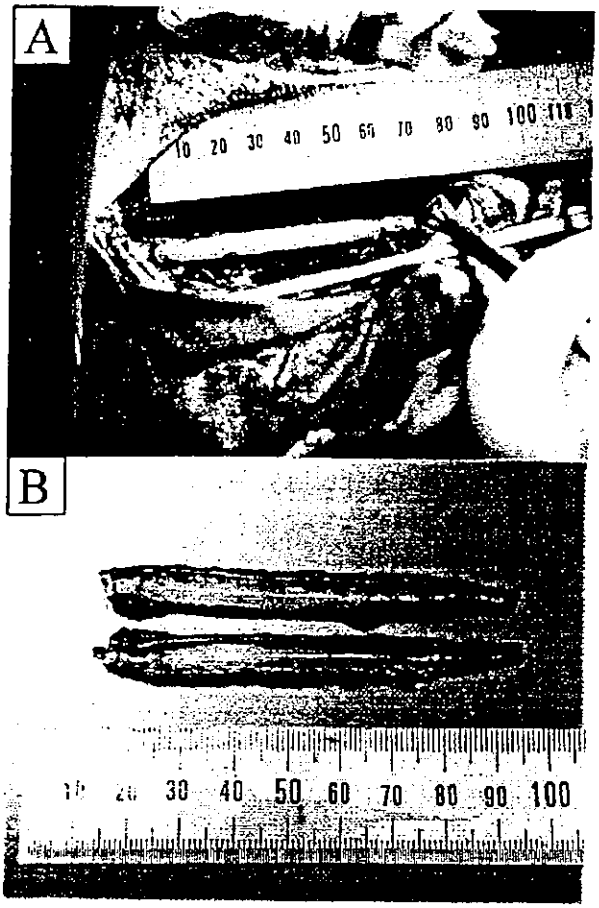

Figure 5. Macroscopic examination of EPC-seeded vascular grafts: *A*, as implanted; *B*, the grafts had a smooth, glistening, and ivory-colored luminal surface 3 months after implantation.

TABLE 1. Patency versus implantation period

Implantation period (mo)	No. of implanted grafts
1	6 (1)*
3	6 (0)

*Number in parentheses represents the number of dilated or occluded grafts.

further cultured for 1 week. The graft (dimensions of approximately 4.5 mm in diameter and 6 cm in length) was connected to the carotid arteries of a dog from which peripheral blood was withdrawn (Figure 5, *A*). There was neither dilation along the graft nor stricture at either anastomostic site at implantation. The projected implantation period was scheduled to occur at 1 and 3 months. Eleven of 12 implanted grafts were completely patent. The smooth, glistering, ivory-colored luminal surfaces, which are free of thrombus, were observed for completely patent grafts at 3 months after implantation (Fig 5, *B*). One graft at 1 month after implantation was dilated and partially occluded by the thrombus, which might be due to loosening of the wrapping sutures along the graft. The overall results of the implanted grafts are summarized in Table 1.

Scanning electron microscopic observation showed that the luminal surfaces of the grafts at 3 months after implantation were covered with a confluent monolayer of cobblestone-like cells oriented parallel to the direction of arterial flow (Figure 6, *A* and *B*). Immunohistologically, monolayered cells on the luminal surface of the graft were positive for the factor VIII–related antigen, as shown in Figure 7, *A*. The ingrowth of the surrounding connective tissue through the pores of the wrapping material was distinct (Figure 7, *B*): cells strongly stained with anti-vimentin, probably identified as fibroblasts, invaded the pore in up to two thirds of the neoarterial tissue and the thin layer in the luminal region. Cells (defined as smooth muscle cells) positively stained with smooth muscle cell–specific α-actin, were observed, with accumulation in the subtissue beneath the luminal surface and distribution in the middle part of the neoarterial tissue (Figure 7, *C*). Figure 8 shows a typical morphogenetic feature of the tissue stained with hematoxylin and eosin (cells), Masson trichrome (collagen), and Alcian blue (proteoglycan), indicating that tissue regeneration proceeded well. The neoarterial walls have a thickness of less than 200 μm at 1 month after implantation and approximately 300 μm at 3 months after implantation (Figure 9). For both cases, there is little distance dependency of neoarterial tissue formation (from the anastomotic site).

Discussion

Although extensive efforts have been made to develop a vital, functioning, small-diameter artificial graft (inner diameter of <5 mm), none have been realized clinically. On the other hand, EC transplantation onto a synthetic artificial graft by using either seeding or sodding techniques has exhibited proved nonthrombogenic potential once a fully endothelial monolayer that can withstand high pressure–loaded arterial circulatory stress is formed on the luminal surface of the artificial graft.[1] Early successes achieving long-term patency of EC-lined small-diameter grafts in animal studies have not been followed by extensive use of this technology in human subjects, except for by Zilla's group, who have been extensively implanting EC-seeded grafts under well-defined clinical criteria and surgical procedures and reported a more than 9-year follow-up study. The major reasons for limited clinical realization must be the limited number of ECs that can be obtained from a segment of autologous vein, as well as questions concerning the removal of viable vein segments from patients with vascular diseases.

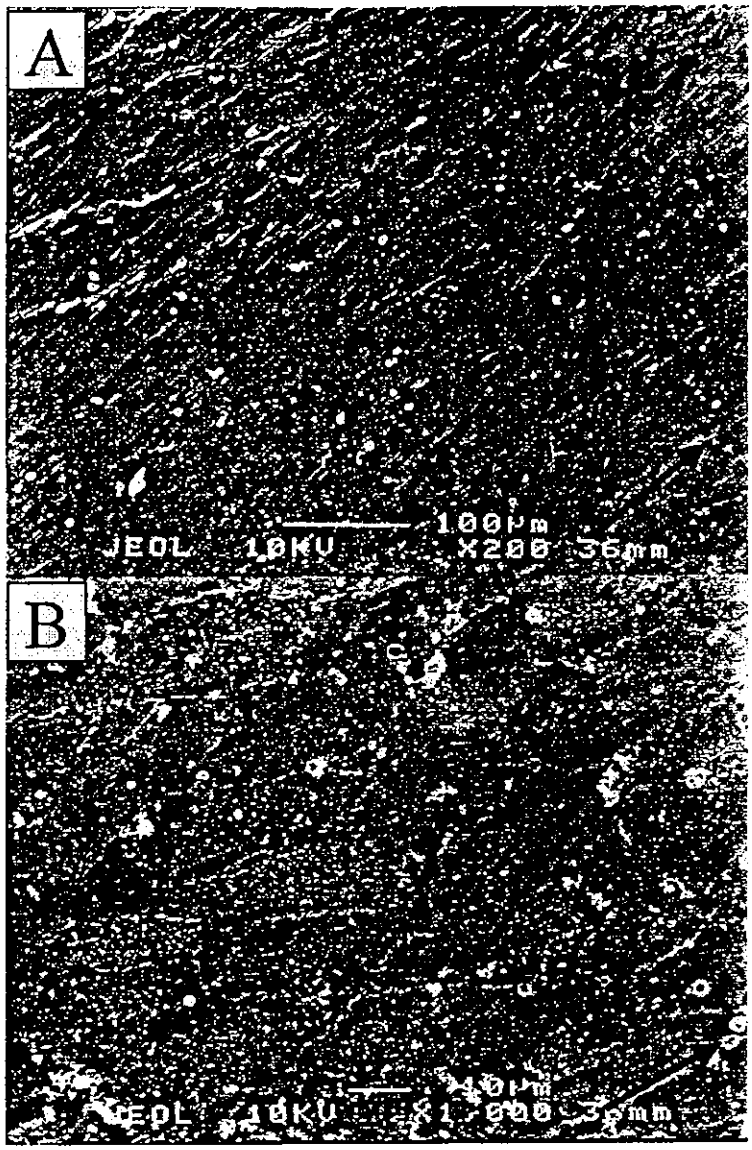

Figure 6. Scanning electron micrographic examination of the luminal surface of the graft 3 months after implantation. The intima was covered with a confluent endothelial monolayer oriented parallel to the direction of arterial blood flow. (Original magnification: *A*, 100×; *B*, 1000×.) *Arrows* indicate the direction of arterial blood flow.

Alternative sources of autologous ECs are omental fat[14] or adipose tissues.[15] ECs from omental microvascularized fat on an artificial graft have experimentally contributed to endothelialization. However, it has been suggested that microvascular ECs from omental tissue are not of endothelial origin.[16] Sodding of fragmented vessel tissues has been clinically used in Japan. On implantation, in situ cell sorting resulted in the formation of EC lining on subvascular tissue with implantation time.[17] However, this method might not be applicable to a small-diameter graft because massive thrombus is formed at a very early phase of implantation.[18]

Recent studies have shown that mature fall-out ECs detached from the vascular wall and bone marrow–derived EPCs are circulating in the peripheral bloodstream.[2-5] A very small amount of bone marrow–derived EPCs circulating in blood, which are differentiated from $CD34^+$ cells, form endothelial colonies.[3-5,19] These cells uptake acetylated low-density lipoprotein, produce NO by means of vascular endothelial growth factor stimulation, and express von Willebrand factor, vascular endothelial cadherin, platelet endothelial cell adhesion molecule 1, vascular endothelial growth factor receptor 2 (Flk-1), and Tie-2 receptor.[2,3,20]

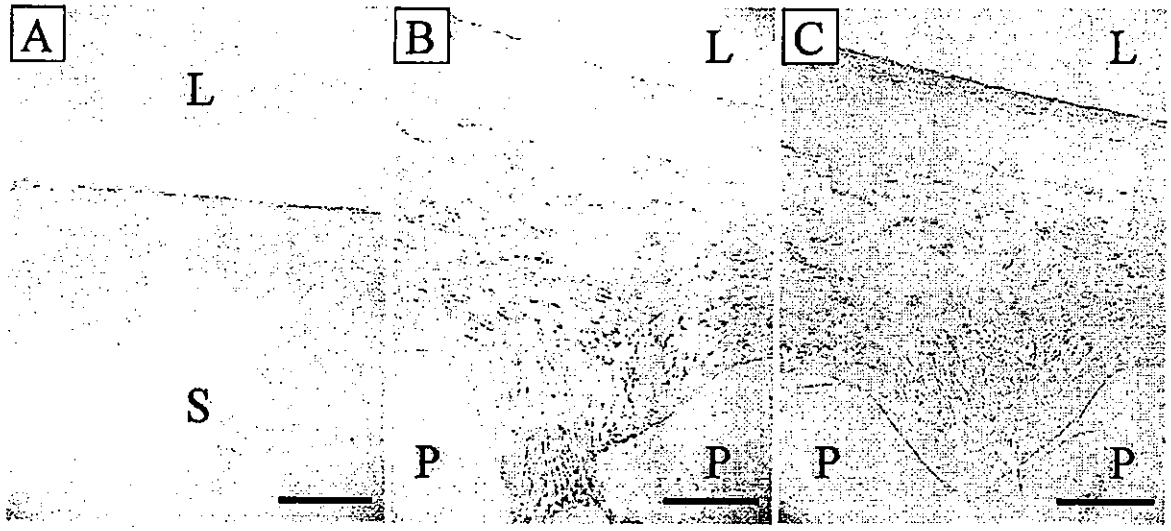

Figure 7. Immunochemical staining of the neoarterial wall of EPC-seeded vascular grafts 3 months after implantation: *A*, monoclonal antibody against factor VIII–related antigen (original magnification 200×); *B*, monoclonal antibody against vimentin (original magnification 200×); *C*, monoclonal antibody against smooth muscle α-actin (original magnification 200×). *L*, Luminal surface; *S*, SPU-contacting surface; *P*, wrapped polyurethane. *Scale bars* = 100 μm.

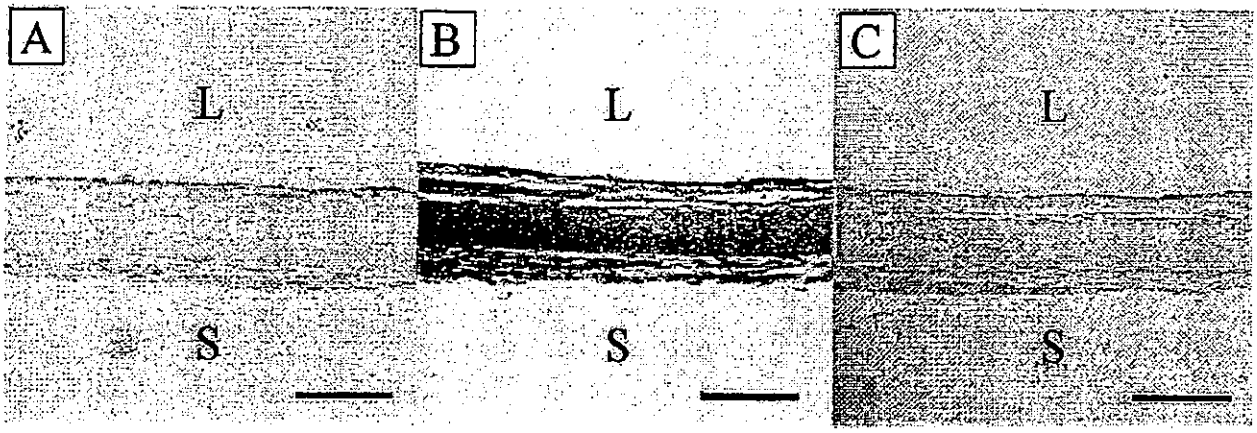

Figure 8. Histologic examination of the neoarterial wall of EPC-seeded vascular grafts 3 months after implantation (original magnification 200×): *A*, hematoxylin and eosin staining; *B*, Masson trichrome staining; *C*, Alcian blue staining. *L*, Luminal surface; *S*, SPU-contacting surface. *Scale bars* = 100 μm.

Before the existence of EPCs in circulating blood was scientifically defined, several articles reported that implanted artificial devices were endothelialized for a long period in vivo. The contribution of such ECs or EPCs to endothelialization on impervious artificial grafts and ventricular assist devices, both of which totally prevent transinterstitial tissue ingrowth, was observed in canine and sheep models, respectively. Shi and coworkers[6] reported that scattered islands of endothelial-like cells and α-actin–positive smooth muscle cells were found beneath some of the endothelial islands on the artificial graft. In addition, Frazier and associates[21] reported neointima that formed on the surface of left ventricular assist devices is colonized by $CD34^+$ cells.

Our separate study with human EPCs revealed that antiplatelet activity, as determined quantitatively on the basis of the production rate of endothelial-type NO synthase and prostacyclin, and fibrinolytic activity, as determined on the basis of the production rate of the tissue plasminogen activator, were almost one third to one half of the former

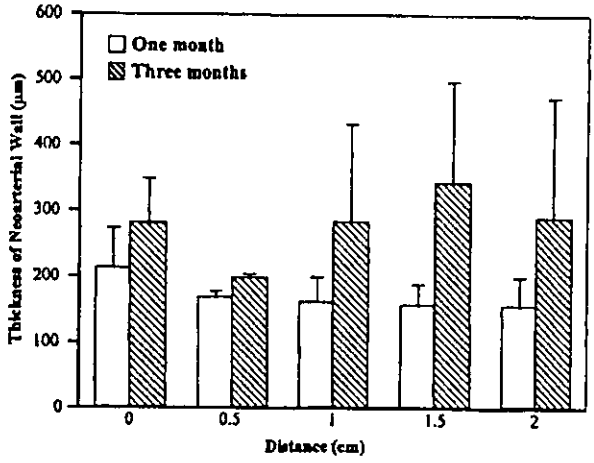

Figure 9. Thickness of neoarterial wall as a function of distance from distal anastomotic site 1 and 3 months after implantation. Each result is expressed as the mean ± SD.

activity of human ECs and almost equivalent for the latter.[22] Therefore human EPCs might have nonthrombogenicity close to that of ECs.

In this study canine EPCs harvested from circulating peripheral blood and cultured according to a method similar to that previously reported[22] were obtained at a harvesting rate of approximately 15% on single (15 mL of blood) or multiple sampling. (Note that this rate is very high compared with approximately 18% for human EPCs from 100 mL of blood, as shown in our experiment.[22]) The uptake of low-density lipoprotein, the expression of factor VIII and Flk-1, and the production of intracellular NO showed that EPCs have the characteristic features of ECs. The patency rate of EPC-based hybrid grafts was almost the same as those of EC-based hybrid grafts, both of which use the same scaffold (microporous SPU tube) and extracellular matrix (collagen meshes).[23] This pulsatile stress-responsive elastomeric tubular scaffold was found to have compliance close to that of canine native carotid arteries, which was investigated in detail in our previous articles.

In situ–formed collagen meshes as a cell-adhering matrix penetrated into and filled micropores of the microporous SPU wall scaffold, thus enabling exertion of the adhesion strength of cell-matrix complexes on the SPU film, which withstands continuously loaded pulsatile stress-inducing hydrodynamic shear stress and mechanical wall distension. The transmural or transinterstitial tissue ingrowth from perigraft tissues through micropores was accompanied with vimentin-positive cells (probably fibroblasts). At 3 months after implantation, smooth muscle cells (α-actin positive cells) were accumulated beneath the luminal surface and scattered distributed in the medial layer. Although we have not yet determined quantitatively the nonthrombogenic potentials of implanted EPCs, EPCs are expected to differentiate into mature ECs as the implantation period proceeds. This means that EPCs existing in circulating peripheral blood can be an alternative cell source for vascular tissue–engineered grafts. In fact, recent clinical studies have shown that the infusion of the mononuclear cell fraction or $CD34^+$ cells, both of which contain EPCs, into ischemic tissues in legs markedly improved the blood circulation in peripheral regions caused by vasculogenesis.[24] On the other hand, a recent study of ovine EPC–seeded decellularized porcine iliac vessels exhibited high patency, as well as contractile activity and NO-mediated vascular relaxation, similar to that of native arteries.[8] Thus on the basis of these preceding studies, EPC-based engineered grafts are clinically promising. Because isolation of EPCs and their mass proliferation is a critical task for such an engineered graft, harvesting from a patient's bone marrow by mobilizing with the aid of colony-stimulating factor and isolation and clonal proliferation of EPCs is more suited than those from peripheral blood.

Dr He is on leave of absence from the Zhujiang Hospital affiliated to the First Military Medical University of PLA, P.R. China.

References

1. Deutsch M, Meinhart J, Fischlein T, Preiss P, Zilla P. Clinical autologous in vitro endothelialization of infrainguinal ePTFE grafts in 100 patients: a 9-year experience. *Surgery.* 1999;126:847-55.
2. Asahara T, Murohara T, Sullivan A, Silver M, van der Zee R, Li T, et al. Isolation of putative progenitor endothelial cells for angiogenesis. *Science.* 1997;275:964-7.
3. Shi Q, Rafii S, Wu MH, Wijelath ES, Yu C, Ishida A, et al. Evidence for circulating bone marrow–derived endothelial cells. *Blood.* 1998; 92:362-7.
4. Lin Y, Weisdorf DJ, Solovey A, Hebbel RP. Origins of circulating endothelial cells and endothelial outgrowth from blood. *J Clin Invest.* 2000;105:71-7.
5. Peichev M, Naiyer AJ, Pereira D, Zhu Z, Lane WJ, Williams M, et al. Expression of VEGFR-2 and AC133 by circulating human CD34(+) cells identifies a population of functional endothelial precursors. *Blood.* 2000;95:952-8.
6. Shi Q, Wu MH, Hayashida N, Wechezak AR, Clowes AW, Sauvage LR. Proof of fallout endothelialization of impervious Dacron grafts in the aorta and inferior vena cava of the dog. *J Vasc Surg.* 1994;20:546-57.
7. Shi Q, Wu MH, Fujita Y, Ishida A, Wijelath ES, Hammond WP, et al. Genetic tracing of arterial graft flow surface endothelialization in allogeneic marrow transplanted dogs. *Cardiovasc Surg.* 1999;7:98-105.
8. Kaushal S, Amiel GE, Guleserian KJ, Shapira OM, Perry T, Sutherland FW, et al. Functional small-diameter neovessels created using endothelial progenitor cells expanded ex vivo. *Nat Med.* 2001;7:1035-40.
9. Kojima H, Nakatsubo N, Kikuchi K, Kawahara S, Kirino Y, Nagoshi H, et al. Detection and imaging of nitric oxide with novel fluorescent indicators: diaminofluoresceins. *Anal Chem.* 1998;70:2446-53.
10. Zilla P, Fasol R, Dudeck U, Siedler S, Preiss P, Fischlein T, et al. In situ cannulation, microgrid follow-up and low-density plating provide first passage endothelial cell mass cultures for in vitro lining. *J Vasc Surg.* 1990;12:180-9.
11. He HB, Matsuda T. Newly designed compliant hierarchic hybrid vascular graft wrapped with microporous elastomeric film (II): morphogenesis and compliance change upon implantation. *Cell Transplant.* 2002;11:75-87.

12. Doi K, Nakayama Y, Matsuda T. Novel compliant and tissue-permeable microporous polyurethane vascular prosthesis fabricated by an excimer laser ablation technique. *J Biomed Mater Res.* 1996;31:27-33.
13. Kobashi T, Matsuda T. Branched hybrid vessel: in vitro loaded hydrodynamic forces influence the tissue architecture. *Cell Transplant.* 2000;9:93-105.
14. Jarrell BE, Williams SK, Stokes G, Hubbard FA, Carabasi RA, Koolpe E, et al. Use of freshly isolated capillary endothelial cells for the immediate establishment of a monolayer on a vascular graft at surgery. *Surgery.* 1986;100:392-9.
15. Kern PA, Knedler A, Eckel RH. Isolation and culture of microvascular endothelium from human adipose tissue. *J Clin Invest.* 1983;71:1822-9.
16. Visser MJ, van Bockel JH, van Muijen GN, van Hinsbergh VW. Cells derived from omental fat tissue and used for seeding vascular prostheses are not endothelial in origin. A study on the origin of epitheloid cells derived from omentum. *J Vasc Surg.* 1991;13:373-81.
17. Karube N, Soma T, Noishiki Y, Yamazaki I, Kosuge T, Ichikawa Y, et al. Clinical long-term results of vascular prosthesis sealed with fragmented autologous adipose tissue. *Artif Organs.* 2001;25:218-22.
18. Noishiki Y, Tomizawa Y, Yamane Y, Okoshi T, Satoh S, Matsumoto A. Acceleration of neointima formation in vascular prostheses by transplantation of autologous venous tissue fragments. Application to small-diameter grafts. *J Thorac Cardiovasc Surg.* 1993;105:796-804.
19. Boyer M, Townsend LE, Vogel LM, Falk J, Reitz Vick D, Trevor KT, et al. Isolation of endothelial cells and their progenitor cells from human peripheral blood. *J Vasc Surg.* 2000;31:181-9.
20. Murohara T, Ikeda H, Duan J, Shintani S, Sasaki K, Eguchi H, et al. Transplanted cord blood-derived endothelial precursor cells augment postnatal neovascularization. *J Clin Invest.* 2000;105:1527-36.
21. Frazier OH, Baldwin RT, Eskin SG, Duncan JM. Immunochemical identification of human endothelial cells on the lining of a ventricular assist device. *Tex Heart Inst J.* 1993;20:78-82.
22. Shirota T, He HB, Yasui H, Matsuda T. Human endothelial progenitor cell (EPC)–seeded hybrid graft: proliferative and antithrombogenic potentials in vitro and fabrication processing. *Tissue Eng.* 2003;9:127-36.
23. Matsuda T, Miwa H. A hybrid vascular model biomimicking the hierarchic structure of arterial wall. neointimal stability and neoarterial regeneration process under arterial circulation. *J Thorac Cardiovasc Surg.* 1995;110:988-97.
24. Tateishi E, Masaki H, Matsubara H. Clinical feasible therapeutic angiogenesis using autologous implantation of bone marrow-derived mononuclear cells to ischemic limbs [abstract]. *Jpn Circ J.* 2001; 65(suppl 1-A):181.

Novel therapeutic strategy for prevention of malignant tumor recurrence after surgery: Local delivery and prolonged release of adenovirus immobilized in photocured, tissue-adhesive gelatinous matrix

Hidenobu Okino,[1,2] Tatsuya Manabe,[1,2] Masao Tanaka,[1] Takehisa Matsuda[2]
[1]*Department of Surgery and Oncology, Graduate School of Medicine, Kyushu University, 3-1-1 Maidashi, Higashi-ku, Fukuoka 812-8582, Japan*
[2]*Department of Biomedical Engineering, Graduate School of Medicine, Kyushu University, 3-1-1 Maidashi, Higashi-ku, Fukuoka 812-8582, Japan*

Received 4 April 2002; revised 16 October 2002; accepted 8 November 2002

Abstract: We have been developing a new gene delivery method using a styrenated gelatin-based tissue-adhesive matrix that allows *in situ* adenovirus-immobilized gel formation on living tissue and sustained virus release to permeate carcinoma tissue. Styrenated gelatin was synthesized by the condensation reaction of gelatin with 4-vinylbenzoic acid. Aqueous styrenated gelatin solution premixed with AdLacZ, adenovirus encoding β-galactosidase cDNA, and carboxylated camphorquinone (CQ) as a photoinitiator was irradiated with visible light to form a styrenated gelatin gel. The *in vitro* adenovirus release from the styrenated gelatin gel to a medium strongly depended not on styrenated gelatin concentration but on CQ concentration. Maximal β-galactosidase expression was observed on day 1, followed by a rapid decrease that continued up to 1 month for a styrenated gelatin gel prepared with a low styrenated gelatin concentration and a low CQ concentration. Dose-dependent reduced expression of β-galactosidase activity with increasing CQ under photoirradiation was observed. AdLacZ-immobilized styrenated gelatin gel was formed on a hybrid tissue, which is a cell traction-induced collagenous gel entrapped with fibroblasts, and lacZ gene expression of fibroblasts in the hybrid tissue was observed for more than one month. The result of this *in vitro* model experiment implies that the tissue-adhesive styrenated gelatin may be applicable for the delivery of adenovirus encoding cDNA for tumor dormancy therapy into malignant tissue to prevent tumor recurrence after surgery when cDNA is properly selected. © 2003 Wiley Periodicals, Inc. J Biomed Mater Res 66A: 643–651, 2003

Key words: styrenated gelatin; adenovirus; delivery system

INTRODUCTION

A therapeutic procedure leading to avoid recurrence of malignant tumors after radical operation cannot be realized by surgery alone, and a new therapeutic strategy has been long awaited. Our concept to this end is based on the *in situ* construction of a tissue-adhesive local delivery system of bioactive substance for the surgically injured tissue after removal of malignant tissue. The feature of our local delivery system is visible-light–induced radical polymerization of styrenated gelatin, which is photocured to form a gelatinous matrix and drug-immobilized reservoir and from which an anticancer substance is slowly released with time for permeation into the deeper region of the target diseased tissue.

In our previous study,[1] such an *in situ* photocuring system was extensively investigated in terms of the release of proteinaceous drugs and its controlling factors. The latter systems include material parameters (degree of styrene groups in a gelatin molecule) and operation parameters (concentrations of both styrenated gelatin and radical initiator), both of which eventually control the release rate, the release period, tissue adhesivity, photocuring rate, and applied viscosity. In fact, a viscous-buffered solution optimally formulated with styrenated-gelatin–based tissue adhesive and a proteinaceous model drug was rapidly

Correspondence to: T. Matsuda; e-mail: matsuda@med.kyushu-u.ac.jp
Contact grant sponsor: Promotion Fundamental Studies in Health Science of the Organization for Pharmaceutical Safety and Research (OPSR); contact grant number: 97-15
Contact grant sponsor: Scientific Research from Ministry of Education, Culture, Sports, Science, and Technology of Japan; contact grant number: A2-12358017 and B2-12470277

converted to a gel with visible-light irradiation and exhibited prolonged delivery of the drug to living tissue.

The present study is an extension of our previous study of the local delivery system and focuses on the immobilization of a gene-encoding adenovirus and its release from the photocured gelatinous matrix. Regardless of the synthetic drug, protein or gene-encoding adenovirus, our technology based on the *in situ* photopolymerization technique shows many advantages for the following reasons. First, the desired amount of adenovirus in a photocurable gelatinous matrix can be easily immobilized. Second, the crosslinking density, which may affect the adenovirus-release rate, can be controlled. Third, *in situ* photopolymerization allows the creation of a local reservoir and release site of adenovirus on a target tissue.

In the first part of this article, the immobilization of adenovirus in the photocured gel formed with visible-light irradiation and the sustained release of adenovirus are described. Then, we discuss the feasibility of adenovirus-mediated gene transfer from gelatinous matrix to hybrid tissues.

MATERIALS AND METHODS

Preparation of styrenated gelatin

The synthesis and characterization of styrenated gelatin (M_w: 9.5×10^4) and a carboxylated camphorquinone (CQ) and the photogelation method were described in detail in our previous work.[2]

Gel yield and degree of swelling

Gel yield and degree of swelling were measured according to the method previously reported.[1] Gel yield (%) was calculated using the equation $W_{gel}/W_{solid} \times 100$, and the degree of swelling (DS) was calculated as $(W_{water} - W_{gel})/W_{gel}$ (W_{solid}: the weight of solid content in styrenated gelatin gel, W_{water}: the weight of swollen styrenated gelatin gel in water, and W_{gel}: the weight of vacuum-dried styrenated gelatin gel).

Replication-defective recombinant adenovirus

Replication-defective E1a, E1b, and E3 recombinant adenovirus vector expressing *Esclierichia coli* lacZ (AdLacZ) was kindly gifted from Professor H. Ueno (University of Occupational and Environmental Health, Fukuoka, Japan).[3,4] The titer of the viral stock was assessed by a plaque formation assay using 293 cells and expressed as a plaque-forming unit (pfu).

Preparation of aqueous styrenated gelatin solution and photoirradiation

Sorbitol-added lactated Ringer's solution (Otsuka Pharmaceuticals, Tokushima, Japan) containing AdLacZ, styrenated gelatin, and CQ was vigorously mixed with a high-speed rotary shaker. Visible-light irradiation was conducted using an 80 W halogen lamp (Tokuso power lite, Tokuyama Co., Ltd., Tokuyama, Japan; wavelength: 400 to 520 nm, light intensity: 1.3×10^6 lux).

Determination of adenovirus release

Two hundred milligrams of AdLacZ (8.18×10^8 pfu)-containing styrenated gelatin solution was added to the each well of a 24-well microplate (Corning Incorporated, Corning, NY) and subsequently irradiated with visible-light for 3 min to form a styrenated gelatin gel. Two milliliters of Dulbecco's modified Eagle medium (DMEM, Gibco Laboratories Inc., Grand Island, NY) supplemented with 10% fetal bovine serum (FBS, CSL Ltd., Victoria, Australia) was added to each well and the medium was withdrawn at regular intervals. A microplate assay using the fluorescent dye, PicoGreen (Molecular Probes, Eugene, OR), was used to quantify the released adenovirus DNA according to the method previously reported.[5] The microplate was read on an imaging analyzer (Molecular imager FX, Bio-Rad, Hercules, CA) with excitation and emission settings of 488 and 530 nm, respectively.

Cell line

MRC-5, a potent hepatocyte growth factor (HGF) producing fibroblast cell line, was obtained from the American Type Culture Collection (Rockville, MD) and maintained in DMEM supplemented with 10% FBS, 100 U/mL streptomycin, and 100 U/mL penicillin.

Quantitation of β-galactosidase expression

Fibroblasts (MRC-5: density of 1×10^4 cells/cm^2) were cultured in 2 mL of DMEM supplemented with 10% FBS in which an AdLacZ (8.18×10^8 pfu)-immobilized styrenated gelatin gel was soaked. Two days later, the lacZ expressions of the fibroblasts were quantified by measuring &gr;-galactosidase activity by means of a calorimetric assay using *O*-nitrophenyl-β-D-galactopyranoside (Sigma-Aldrich Co., St. Louis, MO) as previously described[6] using a microplate reader (Microplate Reader 550, Bio-Rad) at 415 nm.

Contact effect of adenovirus with photocured gel and unreacted styrenated gelatin

Two hundred milligrams of the styrenated gelatin solution (phosphate-buffered saline (Dainippon Pharmaceutical

Co., Ltd., Osaka, Japan; styrenated gelatin concentration: 20 or 30 wt %, CQ concentration: 0.05 wt %) was at first photocured on the each well of a 12-well microplate (Corning), and 2 mL of AdLacZ solution (titer: 6.82×10^9 pfu/mL) was subsequently added to the each well. After shaking on a shaker (Mild Mixer PR-36, TAITEC, Saitama, Japan) for 6 h, AdLacZ solution was withdrawn and added to a medium, DMEM supplemented with 10% FBS [at a multiplicities of infection (moi) of 10 to 50], and then fibroblasts (MRC-5) were cultured with the medium at a density of 1×10^4 cells/cm^2. Separately, fibroblasts (MRC-5) were also cultured in the medium mixed with AdLacZ solution and 20 wt % unreacted styrenated gelatin at an moi of 10 to 50. Two days later, the lacZ expressions of the fibroblasts were quantified by a calorimetric assay.[6]

Effect of camphorquinone on adenovirus DNA

CQ (concentration: 0.1 to 1.0 wt % based on the weight of AdLacZ solution) was added to the AdLacZ solution (1.71×10^9 pfu) with or without visible-light irradiation for 3 min (light intensity: 1.3×10^6 lux). DNA of AdLacZ was extracted with the use of a QIAamp DNA Mini kit (Qiagen, Hilden, Germany) following the manufacturer's instruction. Ten microliters of the extracted products was subjected to electrophoresis (FIGE Mapper System, Bio-Rad) in 1% agarose gel and stained by ethidium bromide (Sigma-Aldrich Co.). The relative fluorescence intensities of the DNA bands were measured by an imaging analyzer (Molecular imager FX, Bio-Rad) with excitation and emission settings of 532 and 555 nm, respectively.

Gene transduction in tissue

A disc-type hybrid tissue (diameter: 10 mm, thickness: 1 mm) as an *in vitro* tissue model was prepared with a DMEM solution containing fibroblasts (MRC-5; 5×10^4 cells) and type I collagen (0.3%; Cellgen, Koken Corp., Tokyo, Japan), subsequently incubated at 37°C, followed by incubation for 7 days according to the method previously described.[7] Twenty milligrams of 20 or 30 wt % styrenated gelatin solution premixed with AdLacZ (8.18×10^7 pfu) was coated on the tissue surface and subsequently irradiated with visible light to form a styrenated gelatin gel. Transverse cryostat sections prepared with a microslicer (CM 1850, Leica, Nussloch, Germany) were subjected to X-gal staining with chromogenic substrate, 5-bromo-4-chloro-3-indolyl-β-galactopyranoside (Sigma-Aldrich Co.), according to the method previously described[8] and observed under a phase-contrast microscope (TE 300, Nikon, Tokyo, Japan).

RESULTS

Gel yield and degree of swelling

The viscous mixture of styrenated gelatin (27.6 styrene groups per gelatin molecule), a CQ as a photoinitiator and AdLacZ as a model DNA-encoding adenovirus was photocured to form a styrenated gelatin gel by visible light-induced radical polymerization of the styrene groups. Two different concentrations of styrenated gelatin were used: 20 and 30 wt %. CQ concentration ranged from 0.05 to 2 wt % based on the weight of styrenated gelatin. Figure 1 shows the effects of CQ concentration on gel yield. Gel yield and equilibrium degree of swelling (DS) were independent of CQ concentration, regardless of the concentration of styrenated gelatin (Fig. 1). Gel yield was approximately 55–75%, and DS was approximately 9–12. The high styrenated gelatin concentration based gel (30 wt % styrenated gelatin gel) gave a slightly higher gel yield but a slightly lower DS than the low styrenated gelatin concentration-based one (20 wt % styrenated gelatin gel; Fig. 1).

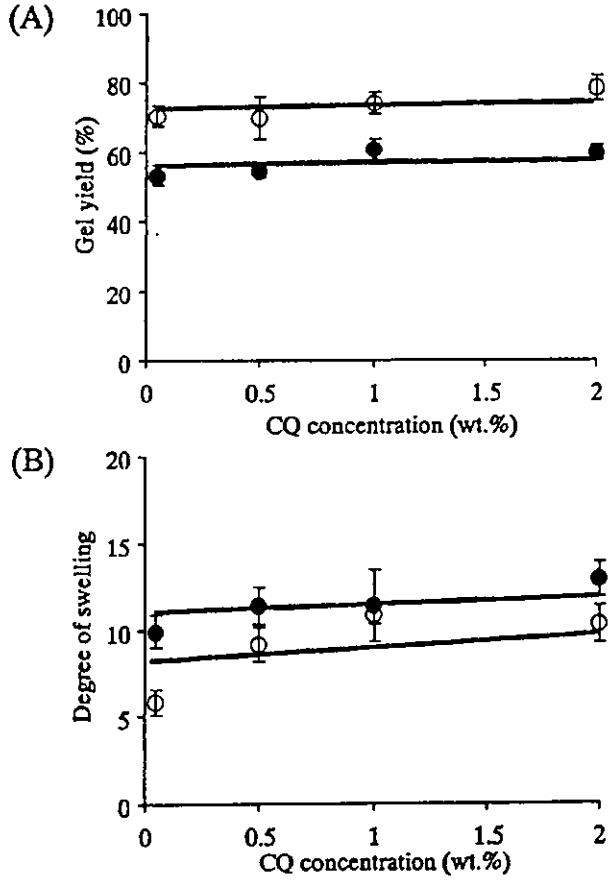

Figure 1. Effects of CQ concentration on gel yield (a) and degree of swelling (b). Gels were prepared with styrenated gelatin at the concentrations of 20 wt% (•) and 30 wt% (○). Values are expressed as mean ± SD (n = 3).

In vitro adenovirus release characteristics

Figure 2 shows the daily and cumulative amounts of AdLacZ released into the medium from styrenated

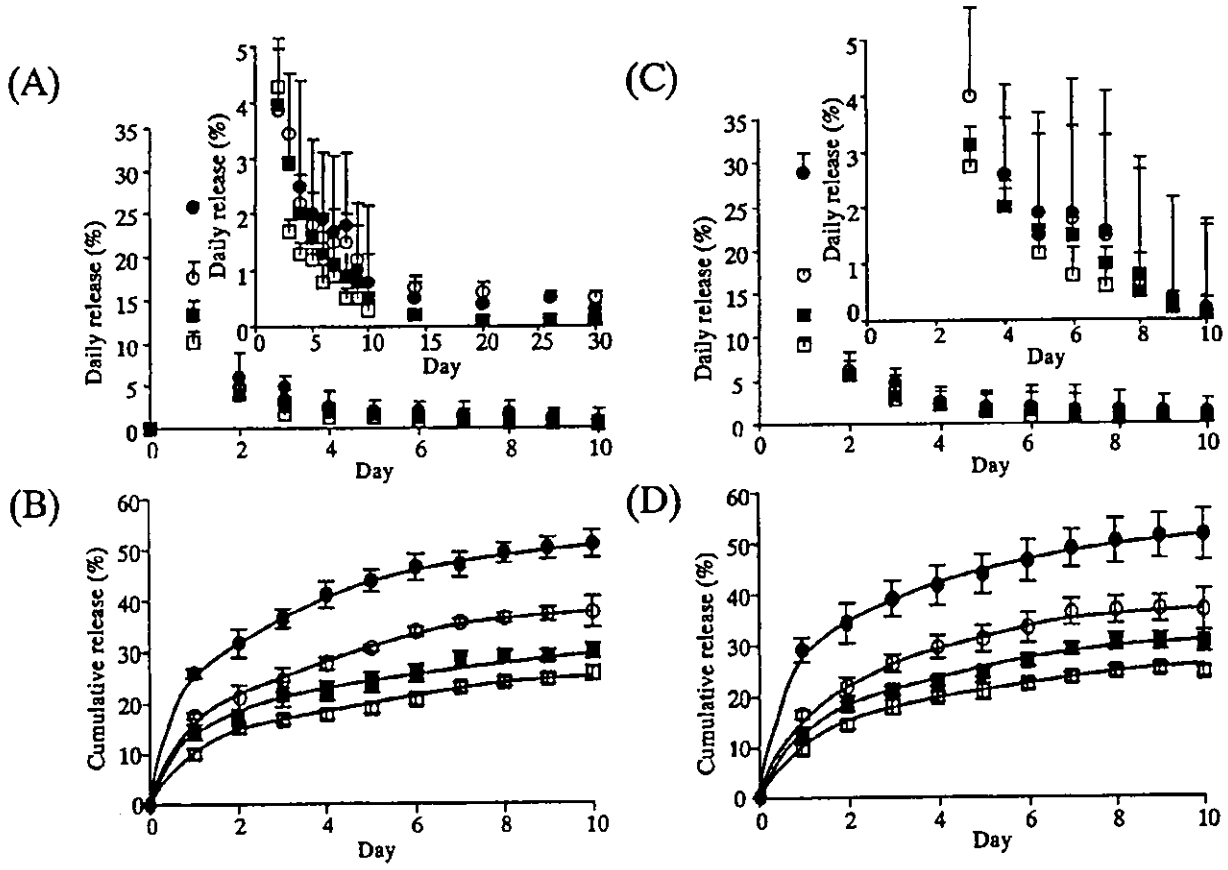

Figure 2. Daily and cumulative amounts of AdLacZ released into the medium from styrenated gelatin gels as a function of incubation time. Gels were prepared with styrenated gelatin at the concentrations of 20 wt % (a,b) and 30 wt % (cd,) with varying CQ concentrations of 0.05 wt % (•), 0.5 wt % (○), 1 wt % (■) and 2 wt.% (□) based on the weight of styrenated gelatin. Values are expressed as mean ± SD (n = 3).

gelatin gels prepared with either 20 or 30 wt % styrenated gelatin and different CQ concentrations, both of which are plotted against the incubation time. Irrespective of the concentrations of styrenated gelatin and CQ, the amount of released adenovirus was the largest on day 1 of incubation and sharply decreased with incubation time, but the release continuously proceeded at a low rate. There is little difference in the release profiles between 20 and 30 wt % styrenated gelatin gels at a fixed CQ concentration; thus, the release rate did not depend on styrenated gelatin concentration. However, the release rate strongly depended on CQ concentration. A lower CQ concentration resulted in a higher release rate, regardless of styrenated gelatin concentration. For example, on day 10 of incubation, approximately 50% of the immobilized adenovirus was released from the styrenated gelatin gel photocured at 0.05 wt % CQ concentration, but only 25% of the adenovirus was released from styrenated gelatin gel prepared at 2 wt % CQ concentration.

Dependence of β-galactosidase expression on styrenated gelatin gel formulation

The β-galactosidase activity of AdLacZ released from a styrenated gelatin gel was assessed in terms of β-galactosidase activity expressed in fibroblasts (MRC-5) that were transfected in the adenovirus-containing medium that was daily collected from the medium contacted with styrenated gelatin gels. The amount of expression of β-galactosidase as detected by calorimetric assay is plotted against the release time (Fig. 3). A marked difference in β-galactosidase expression was observed between the styrenated gelatin gels prepared with different styrenated gelatin concentrations and CQ concentrations. The expression of β-galactosidase for the 20 wt % styrenated gelatin gel was much higher than that for the 30 wt % styrenated gelatin gel (More than a few 10-fold higher expression was noted for the former styrenated gelatin gel compared with the latter one). Higher β-galactosidase activity was observed at a lower CQ concentra-

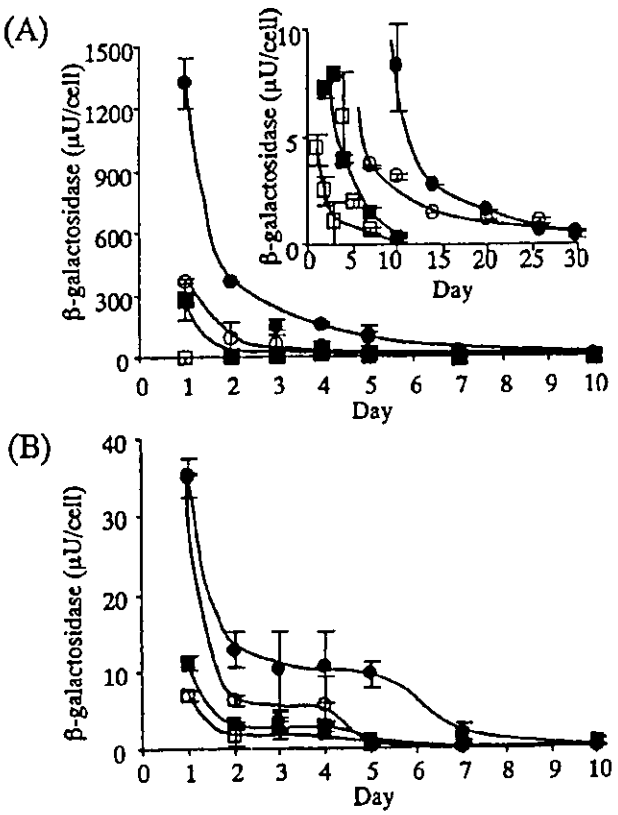

Figure 3. Expression of β-galactosidase was detected by calorimetric assay. Gels were prepared with styrenated gelatin at the concentrations of 20 wt % (a) and 30 wt % (b) with varying CQ concentrations of 0.05 wt % (•), 0.5 wt % (*), 1 wt % (■), and 2 wt % (□) based on the weight of styrenated gelatin. Values are expressed as mean ± SD (n = 3).

tion, regardless of 20 or 30 wt % styrenated gelatin gel. Regardless of styrenated gelatin concentration or CQ concentration, maximal expression of β-galactosidase was observed on day 1, followed by a rapid decrease with time. This tendency resembled that of the daily release characteristics as shown in Figure 2(a,c). Although the expression became weak with time, it continued up to 1 month for some 20 wt % styrenated gelatin gels (CQ concentration less than 0.5 wt %).

Effects of photocured gel and unreacted styrenated gelatin on β-galactosidase expression

To investigate how adenovirus activity was impaired by contacting with styrenated gelatin gel or unreacted styrenated gelatin molecule, AdLacZ solutions were incubated in 20 wt % styrenated gelatin gel and 30 wt % styrenated gelatin gel layered dish or mixed with 20 wt% unreacted styrenated gelatin, both of which were subjected to shaking for 6 h. As control, AdLacZ solution placed in a tissue culture dish was also subjected to shaking for 6 h. As shown in Figure 4, the expression of β-galactosidase largely increased with AdLacZ at low moi and then increased steadily with increasing moi. However, both AdLacZ solutions contacted with 20 wt % styrenated gelatin gel and 30 wt % styrenated gelatin gel showed lower expression of β-galactosidase than that of control, although the expression also increased with an increase in moi. However, AdLacZ solution mixed with 20 wt % unreacted styrenated gelatin molecule showed a marked decrease in expression, regardless of moi. It is apparent that adenovirus bioactivity was almost lost.

DNA integrity

To study the effects of photoirradiation and photoinitiator on the integrity of the adenovirus genome, the adenovirus was incubated with different concentrations of CQ with or without visible-light irradiation, and adenovirus DNA was extracted by filtration according to the manufacturer's instruction. The filtrate was electrophoresed in 1% agarose gel. In the absence of irradiation, the fluorescence intensities of the 35-kb pair bands corresponding to AdLacZ sequences appeared to be almost identical, whereas the fluorescence intensities of the 35-kb pair bands decreased with increasing photoirradiated CQ concentration, although little DNA smear, indicative of random DNA fragmentation, was observed (Fig. 5). This indicates that the DNA content in the filtrate was decreased with an increase in CQ concentration,

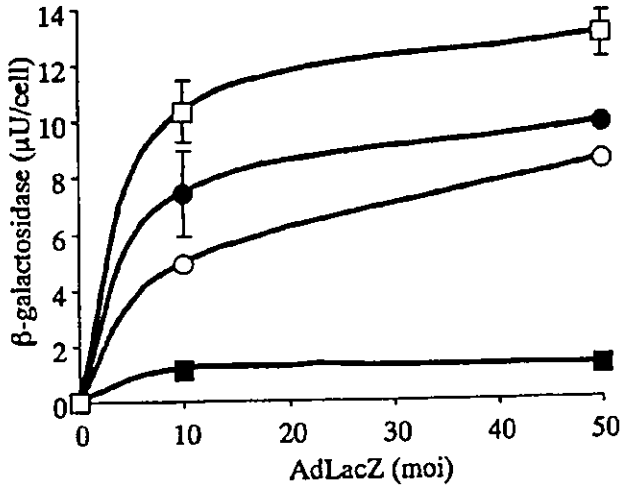

Figure 4. Effect of photocured gel and unreacted styrenated gelatin on β-galactosidase expression. Two milliliters of AdLacZ solution (6.82×10^9 pfu/mL) was contacted with 20 wt % styrenated gelatin gel (•) and 30 wt % styrenated gelatin gel (*) for 6 h on the shaker. Twenty wt % unreacted styrenated gelatin was mixed with AdLacZ solution (■). Control (□). Values are expressed as mean ± SD (n = 3).

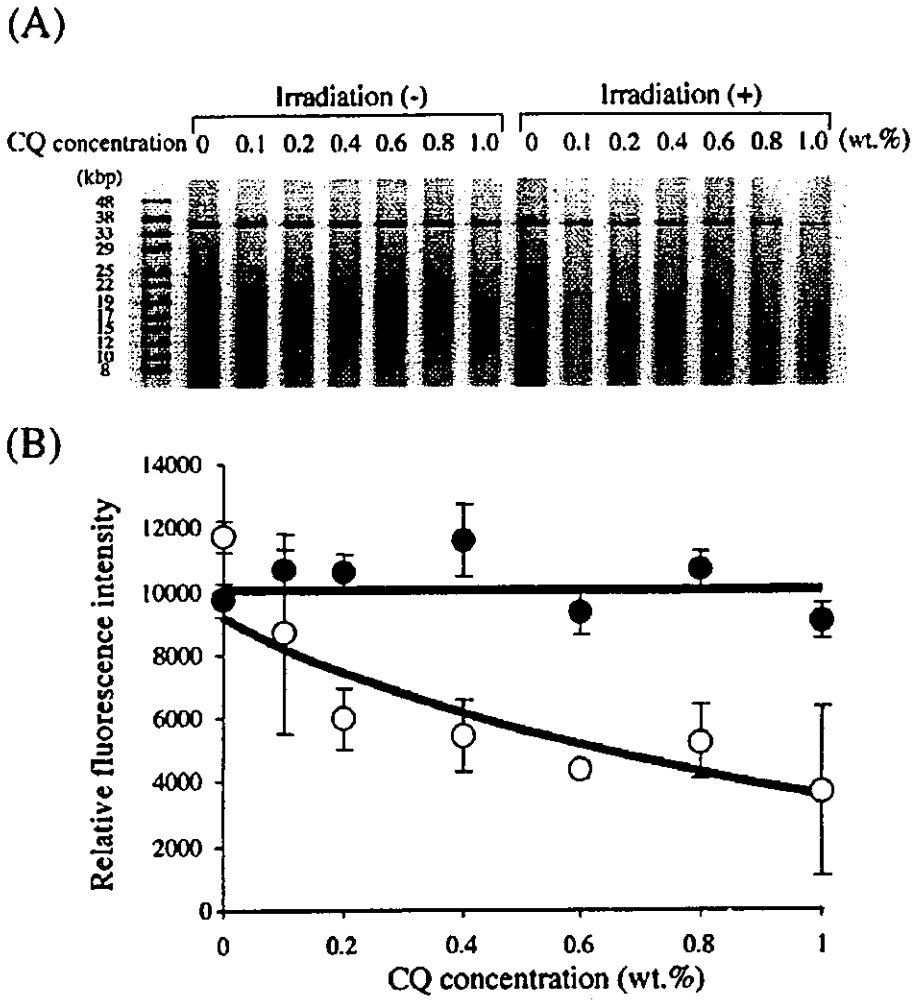

Figure 5. Effect of CQ concentration on adenovirus DNA was examined with or without visible-light irradiation. AdLacZ solution (1.71×10^9 pfu) containing CQ ranging from 0.1 wt % to 1.0 wt % based on solution weight was exposed to visible light at 1.3×10^6 lux for 3 min (a). The relative fluorescence intensity of each DNA band was quantified with irradiation (°) or without irradiation (•) (b). Values are expressed as mean ± SD ($n = 3$).

which may induce adenovirus aggregation via radical reactions due to the photocleaved CQ.

Gene expression in hybrid tissue

Gene transduction from a photocured gel (prepared with 20 wt % styrenated gelatin and 0.05 wt % CQ) to a disc-type hybrid tissue, which is fibroblast-inoculated collagen gel, was conducted as follows. The control group (pretransduction group) was pretransducted with AdLacZ (at an moi of 100) before the fabrication of the hybrid tissue &ls1b;Fig. 6(a)]. X-gal staining-positive cells were observed on day 3 and 7, but did not exist from day 14 onwards in the control group [Fig. 6(a)]. In the *in situ* hydrogelation group, 20 mg of styrenated gelatin solution premixed with AdLacZ (8.18×10^7 pfu) was coated on the hybrid tissue using nontransducted fibroblasts and subsequently irradiated with visible light to form a styrenated gelatin gel [Fig. 6(b)]. The lacZ expression in the hybrid tissue was evaluated over the observation period starting from day 3 to the fourth week by X-gal staining of the transverse section of the tissue [Fig. 6(b)]. The AdLacZ-immobilized styrenated gelatin gels were also stained blue due to the β-galactosidase contained in AdLacZ solution in the virus replication process in 293E1 cell.

DISCUSSION

Our newly developed therapeutic strategy, which uses a styrenated gelatin-based tissue-adhesive matrix that acts as a local reservoir for bioactive substances and

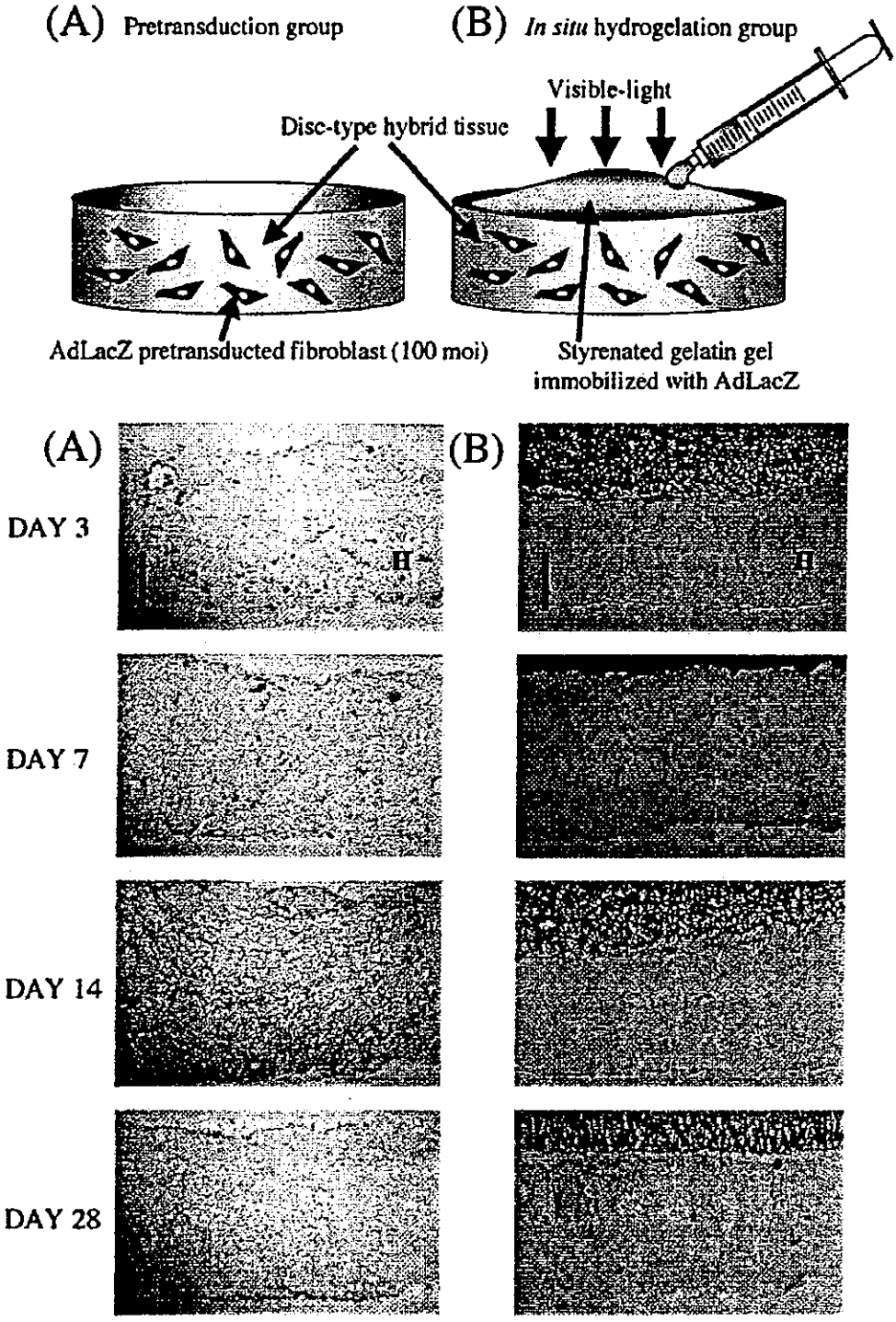

Figure 6. Comparison of the duration of lacZ gene expression using disc-type hybrid tissues. LacZ expressions in the hybrid tissues were evaluated from day 3 to the fourth week by X-gal staining. (a) Pretransucted group. Hybrid tissue was prepared with fibroblasts that were pretransducted with AdLacZ (at an moi of 100) before the fabrication of the hybrid tissue. (b) *In situ* hydrogelation group: Hybrid tissue was coated with 20 mg of styrenated gelatin solution premixed with AdLacZ (8.18×10^7 pfu) and subsequently irradiated with visible-light to form a styrenated gelatin gel. G, styrenated gelatin gel immobilized with AdLacZ; H, hybrid tissue. Bar = 200 μm, ×100.

adheres to the target tissue, involves the immobilization and release of adenovirus encoding cDNA for tumor dormancy therapy *in situ* at the site where an operation for the removal of malignant tissue is conducted. The following results are discussed in respect to the merits and shortcomings of our current technology.

There were only slight differences in gel yield as well as the degree of swelling between the styrenated gelatin gels (20 and 30 wt %), regardless of CQ concentration, although the 20 wt % styrenated gelatin gel exhibited a slightly lower gel yield but a slightly higher degree of swelling than the 30 wt % styrenated gelatin gel [Fig. 1(b)]. It was also found that the adenovirus release rate depended not on styrenated gelatin concentration but on CQ concentration (Fig. 2). A lower CQ concentration led to a higher release rate of adenovirus. We surmise that the radicals produced by photoirradiated CQ may chemically bind adenovirus particles to the styrenated gelatin molecule and the number of bound adenovirus particles may be CQ concentration dependent, thereby resulting in the reduction of the number of releasable adenovirus particles with increasing CQ concentration. Because there is no significant difference in the distribution of voids and micropores between the 20 wt % styrenated gelatin gel and the 30 wt % styrenated gelatin gel in the scanning electron micrograph of photocured styrenated gelatin gel (data not shown), the aforementioned mechanism may operate in this release process.

The reduction of β-galactosidase activity of the AdLacZ solution that was contacted with the styrenated gelatin gel (Fig. 4) implied that "contact inactivation" occurred in adenovirus particles during the processes of adsorption to and desorption from the styrenated gelatin gel. β-Galactosidase activity was markedly reduced when the adenovirus solution was mixed with unreacted styrenated gelatin (Fig. 4) and this might be the result of "complex formation" of adenovirus particles with unreacted styrenated gelatin molecules, thereby reducing virus bioactivity. CQ is considered to be another factor that inactivates the adenovirus. As shown in Figure 5, photoirradiated CQ did not cause the DNA smear (adenovirus double-stranded DNA fragmentation), which indicated the integrity of adenovirus DNA. Adenovirus proteins, such as fiber knob and penton base, which are required for viral entry into target cells,[9–11] might be damaged by photoirradiated CQ (viz crosslinking). Several photosensitizers that produce radicals and subsequent reactive oxygen species with visible-light irradiation have been reported to inactivate the virus bioactivity at the level of DNA and/or virus protein.[12–16] Therefore, we concluded that the synergistic effects of "contact inactivation," "complex formation," and CQ might reduce virus bioactivity under immobilized conditions at both high styrenated gelatin concentrations and high CQ concentrations. It is of importance to discuss on whether CQ and its photodecomposition induce cytotoxicity. In fact, Bryant et al.[17] reported that camphorquinone exhibited concentration-dependent cytotoxicity for NIH/3T3 cells on culture dishes. Our study showed that there is no evidence on hybrid tissues for cytokilling or apoptosis as a result of camphorquinone and its photodecomposition under the experimental condition used in this study (data not shown).

The disc-type hybrid tissue that we have devised to mimic living tissue *in vitro* was covered with AdLacZ-immobilized photocurable gel to estimate the duration of gene expression of adenovirus in tissue. Preliminary studies on the *in vitro* application of AdLacZ-immobilized styrenated gelatin gel to disc-type hybrid tissue resulted in high transduction efficiency and long-term gene expression for at least one month (Fig. 6), indicating that AdLacZ was continuously released from the styrenated gelatin gel for a long period of time. These results suggest that *in situ* gelation technology might overcome the disadvantage of short-term gene expression using adenovirus vector by the continuous release of adenovirus to tissue.

HGF/NK4, which has been recently reported to be an antagonist for HGF, was found to have a potent function to inhibit tumor growth, metastasis and angiogenesis.[18–20] In pancreatic cancer, local recurrence in retroperitoneal space, "tumor bed," after surgery often results in poor prognosis. If the HGF/NK4 gene transduction directly into potentially remnant malignant cells or mesenchymal cells in "tumor bed" after a surgical removal of the primary tumor is feasible using this adenovirus delivery system, it will contribute to the improvement of the prognosis in pancreatic cancer. In the near future, the results of *in vivo* experiments on the inhibition of tumor recurrence using AdNK4-immobilized styrenated gelatin gel will be reported.

References

1. Okino H, Nakayama Y, Tanaka M, Matsuda T. *In situ* hydrogelation of photocurable gelatin and drug release. J Biomed Mater Res 2002;59:233–245.
2. Nakayama Y, Matsuda T. Newly designed hemostatic technology based on photocurable gelatin. ASAIO J 1995;41:374–378.
3. Li J-J, Ueno H, Tomita H, Yamamoto H, Kanegae Y, Saito I, Takeshita A. Adenovirus-mediated arterial gene transfer does not require prior injury for submaximal gene expression. Gene Ther 1995;2:351–354.
4. Li J-J, Ueno H, Pan Y, Tomita H, Yamamoto H, Kanegae Y, Saito I, Takeshita A. Percutaneous transluminal gene transfer into canine myocardium in vivo by replication-defective adenovirus. Cardiovasc Res 1995;30:97–105.
5. Murakami P, McCaman MT. Quantitation of adenovirus DNA and virus particles with the PicoGreen fluorescent Dye. Anal Biochem 1999;274:283–288.
6. Hashimoto M, Aruga J, Hosoya Y, Kanegae Y, Saito I, Mikoshiba K. A neural cell-type-specific expression system using recombinant adenovirus vectors. Hum Gene Ther 1996;7:149–158.
7. Okano T, Matsuda T. Hybrid muscular tissues: preparation of skeletal muscle cell-incorporated collagen gels. Cell Transplant 1997;6:109–118.

8. Price J, Turner D, Cepko C. Lineage analysis in the vertebrate nervous system by retrovirus-mediated gene transfer. Proc Natl Acad Sci USA 1987;84:156–160.
9. Wickham TJ, Mathias P, Cheresh DA, Nemerow GR. Integrins alpha v beta 3 and alpha v beta 5 promote adenovirus internalization but not virus attachment. Cell 1993;73:309–319.
10. Carson SD. Limited proteolysis of the coxsackievirus and adenovirus receptor (CAR) on HeLa cells exposed to trypsin. FEBS Lett 2000;484:149–152.
11. Soudais C, Boutin S, Hong SS, Chillon M, Danos O, Bergelson JM, Boulanger P, Kremer EJ. Canine adenovirus type 2 attachment and internalization: coxsackievirus-adenovirus receptor, alternative receptors, and an RGD-independent pathway. J Virol 2000;74:10639–10649.
12. Schagen FH, Moor AC, Cheong SC, Cramer SJ, van Ormondt H, van der Eb AJ, Dubbelman TM, Hoeben RC. Photodynamic treatment of adenoviral vectors with visible light: an easy and convenient method for viral inactivation. Gene Ther 1999;6: 8737ndash;8781.
13. Abe H, Wagner SJ. Analysis of viral DNA, protein and envelope damage after methylene blue, phthalocyanine derivative or merocyanine 540 photosensitization. Photochem Photobiol 1995;61:402–409.
14. Smetana Z, Ben-Hur E, Mendelson E, Salzberg S, Wagner P, Malik Z. Herpes simplex virus proteins are damaged following photodynamic inactivation with phthalocyanines. J Photochem Photobiol B 1998;44:77–83.
15. Lambrecht B, Mohr H, Knuver-Hopf J, Schmitt H. Photoinactivation of viruses in human fresh plasma by phenothiazine dyes in combination with visible light. Vox Sang 1991;60:207–213.
16. Schnipper LE, Lewin AA, Swartz M, Crumpacker CS. Mechanisms of photodynamic inactivation of herpes simplex viruses: comparison between methylene blue, light plus electricity, and hematoporhyrin plus light. J Clin Invest 1980;65:432–438.
17. Bryant SJ, Nuttelman CR, Anseth KS. Cytocompatibility of UV and visible light photoinitiating systems on cultured NIH/3T3 fibroblasts in vitro. J Biomater Sci Polym Ed. 2000;11:439–457.
18. Date K, Matsumoto K, Shimura H, Tanaka M, Nakamura T. HGF/NK4 is a specific antagonist for pleiotrophic actions of hepatocyte growth factor. FEBS Lett 1997;420:1–6.
19. Kuba K, Matsumoto K, Date K, Shimura H, Tanaka M, Nakamura T. HGF/NK4, a four-kringle antagonist of hepatocyte growth factor, is an angiogenesis inhibitor that suppresses tumor growth and metastasis in mice. Cancer Res 2000;60: 6737–6743.
20. Maehara N, Matsumoto K, Kuba K, Mizumoto K, Tanaka M, Nakamura T. NK4, a four-kringle antagonist of HGF, inhibits spreading and invasion of human pancreatic cancer cells. Br J Cancer 2001;84:864–873.

Artificial Organs
28(1):64–71, Blackwell Publishing, Inc.

Recent Progress of Vascular Graft Engineering in Japan

Takehisa Matsuda

Division of Biomedical Engineering, Graduate School of Medical Sciences, Kyushu University, Fukuoka, Japan

Abstract: The development of a small-diameter vascular graft has long been awaited. This review covers research activities, achievements and progress on vascular engineering in Japan, which was conducted over the last decade. The article includes recently developed experimental scaffolds, biologically active artificial extracellular matrices (ECMs) or non-fouling synthetic coatings, cell sourcing including the autologous vascular cell type, endothelial progenitor cells and genetically-engineered, temporary endothelial-like cells. The discussions were presented from biomechanical, biomaterial, cellular and tissue aspects. Once the mechano-biological and biologically active extracellular milieus are established in a designed vascular graft, the functional, structural and mechanical tissue morphogenesis and adaptation of implanted vascular grafts may proceed with implantation duration, and the spatio-temporal tissue modulations at cytokine, cellular, ECM levels under physiological stress proceed to regenerate vascular tissue architecture. The ultimate solution to a small-diameter vascular graft should be realized by optimal combinations of these factors. **Key Words:** Scaffold—Artificial extracellular matrix—Antithrombogenic coating—Vascular cell type—Vascular tissue engineering.

The development of vitally functioning vascular substitutes has been a more than half-century endeavor. Although medium- to large-diameter artificial grafts made of either expanded poly(tetrafluoroethylene) (ePTFE) tubular sheet or poly(ethylene terephthalate) (PET) fiber fabrics have been enjoying clinical use for many years, however, small-diameter artificial grafts with less than 5–6 mm inner diameter have not yet been realized in clinical settings despite many years of effort and numerous approaches (1). The failure in the early phase of implantation is mainly due to occlusion derived from thrombus formation, which is initiated by foreign surface reactions triggered by highly potent and complex body defense mechanisms, including the participation of humoral systems such as blood coagulation and complement systems, and cellular systems (platelets and white blood cells), followed by continuous tissue ingrowth. In the chronic phase of implantation, an excessive tissue ingrowth (intimal hyperplasia), particularly at the anastomosed site, results in stenosis-induced thrombus formation, and sooner or later the graft is occluded. This is the general scenario of failure for small-diameter grafts. Such stenosis and thrombus formation are not essential problems for medium- to large-diameter grafts, but critical to determining the fate of small-diameter graft implantation.

This article attempts to compile the studies concluded over the last decade on small-diameter artificial and tissue-engineered grafts in Japan. The designs of "mechano-active" and "tissue-permeable" structural scaffold, biological mimicking of an extracellular matrix, and non-fouling coating, cell sourcing are presented first, and various types of engineered tissues are described, followed by a discussion of the promising future direction of small-diameter vascular tissue engineering.

ARTIFICIAL EXTRACELLULAR MATRIX AND ANTITHROMBOGENIC COATING

Non-thrombogenic coatings

A well-defined block copolymer of polystyrene and poly(2-hydroxyethyl methacrylate), which forms a multiphase-separated surface, exhibited non-cell adhesivity for more than 400 days of implantation in a canine model when the block copolymer was

Received September 2003.
Address correspondence and reprint requests to Dr Takehisa Matsuda, Division of Biomedical Engineering, Graduate School of Medical Sciences, Kyushu University, Maidashi 3-1-1, Higashi-ku, Fukuoka 812-8582, Japan. E-mail: matsuda@med.kyushu-u.AC.JP

coated on the luminal surface of the artificial graft to completely fill the pores, thus producing a smooth luminal surface. Neither pannus formation nor tissue ingrowth from the anastomosea sites were observed. Only a very thin proteinaceous layer that did not induce thrombus formation was formed. It has been stated that a well-organized proteinaceous layer on the phase-separated surface is attributed to antithrombogenicity (2,3).

Recently, another approach via a new phospholipid-like polymer coating also provided similar results. A highly antithrombogenic phospholipid polymer, the 2-methacryloyloxyethyl phosphorylcholine (MPC) polymer, has a cell membrane-like structure with potent antithrombogenicity. Coating this polymer on polyester-fabrics luminal surfaces produced non-porous coated grafts. Implanted grafts were thrombus-free, and neither pseudointima nor neointima were formed during one month of implantation in a canine model (4,5).

These two coatings described above, which provided smooth, non-porous surfaces, produced neither neointimal formation nor pannus formation at the anastomosed sites. Therefore, these two studies provide a novel approach to the design of a luminal surface. That is, when the luminal surface is coated with a highly biocompatible polymer that induces the formation of an organized non-thrombogenic proteinaceous layer, such a surface is thrombus-free without endothelialization or transanastomotic and transmural tissue ingrowth. More detailed studies, including long-term performances and surface analyses of implanted small-diameter grafts, are eagerly awaited to elucidate the underlying mechanisms.

Poly(amino acid) urethane copolymer (PAU)

A coating of poly(γ-methyl-glutamate) urethane multiblock copolymer (PAU) on ePTFE converted it from a highly hydrophobic and non-wettable surface to a highly hydrophilic solution surface, while interstices of a graft were maintained similarly to a non-coated one. Such coated ePTFE absorbed water very well. In a rat model rapid transanastomotic endothelialization was observed for a small-diameter (diameter: 1.5 mm) PAU-coated ePTFE vascular graft. Although the research is in a preliminary stage, the interim results look very promising (6).

Photoreactive biomacromolecules

Photoreactive artificial extracellular matrices (ECMs) were designed and tested in vivo. The photoreactive group was derivatized in biomacromolecules including cinnamate, phenylazide and benzophenone. Upon UV irradiation, a pair of associated cinnamate groups was converted to a dimer. The intramolecular dimer formation resulted in the formation of a cross-linked gel. Partially cinnamated biomolecules designed for these purposes were cinnamated hyaluronan (HA) and cinnamated gelatin. The experimental vascular graft, composed of a heparin-immobilized, photocured cinnamated HA gel layer or a luminal surface and a photocured cinnamated gelatin gel layer as an outer coating, was fabricated and implanted in a canine model for a relatively short term. It exhibited a promising result, including a markedly reduced fibrin formation on the luminal surface and enhanced tissue ingrowth from the outer coating. Such a design concept of a differentiated biocompatible surface may be essential for a small-diameter graft (7).

Upon UV-irradiation photolysis, phenylazide and benzophenone produced radicals. Gelatins partially derivatized with either of these photolyzable groups were covalently fixed on the substrate and simultaneously formed a stable gel layer on the substrate due to complex radical reactions. A heparin and basic fibroblast growth factor (bFGF)-coimmobilized gelatinous layer gel thus formed on the luminal surface of a segmented polyurethane (SPU) tube apparently reduced the thrombus formation in an early plase of implantation and markedly enhanced neointimal formation with endothelialization due to bioactive substances-subtained release, as will be described later in detail (8–11).

ARTIFICIAL SCAFFOLD DESIGNS

Major requirements of a scaffold are (1) to be provisional (biodegradable) or permanent (non-biodegradable), depending on the type of application, (2) to enable rapid transmural tissue ingrowth through pores, thus facilitating endothelialization, and (3) to provide a "mechano-active" environment in response to pulsatile stress, resulting in compliance similar to natural vascular grafts. However, currently clinically used artificial grafts, such as ePTFE and polyester-fabric grafts, are so stiff that these grafts hardly inflate, even at a high-pressure region. PET-based fabric grafts, with or without a thin-layer coating of glutaraldehyde-cross-linked gelatin, on the market were made by the Ube company, a Japanese manufacturer. These are the sole commercially available Japan-made grafts which are classified as "non-compliant" vascular grafts.

Porosity

Porosity (the size and density of pores) is a determinant factor for transmural tissue ingrowth;

accompanied by endothelial cells (ECs), it supplies endothelial and endothelium stability due to ensured anchoring of neoarterial tissue, which has been discussed for more than four decades. For example, Wesolowski et al. reported, "Porosity: primary determinant of ultimate fate of synthetic vascular graft" (12) and Fry et al. (13) reported, "Importance of porosity in arterial prostheses". These articles were reported in the early 1960s. The influence of the microfibril length of ePTFE prosthesis upon healing and host modification was studied in detail (14). The lengths of microfibrils studied were 20, 40, 60 and 90 μm. The longer fibril group (60 and 90 μm) provided a much higher degree of endothelialization and a higher volume of collagen produced by cells which invaded through the pores, as compared with the shorter fibril group (20 and 40 μm). This finding is in good accordance with the generally accepted consensus or experimental results that a higher porosity graft exhibits high patency.

Mechano-active environment

Arterial tissues, from the aorta to arterioles, are continuously exposed to dynamic mechanical forces such as perpendicular stress, circumferential stress and shear stress, which are repeatedly driven by cardiac pulsatile output, and these arteries contribute to the efficient forward blood flow to peripheral tissues with minimal energy loss because of their unique biomechanical properties: large inflation in the low-pressure regions, gradually reduced inflation in the physiological pressure regions and little inflation in the high-pressure regions, which is termed the "J" curve in the pressure–diameter plot (15). Among many factors determining the patency of the small-diameter artificial grafts, the compliance mismatch between the native artery and the artificial grafts has been discussed as a major detrimental factor of graft failure of small-diameter artificial grafts. This is due to the fact that thrombus formation and neointimal hyperplasia on the surface of the small-diameter artificial graft are more critical factors for small-diameter graft failure than the medium- to large-diameter artificial grafts, because the effective flow area of the small-diameter artificial graft becomes much smaller when a similar amount of thrombi or a similar degree of neointimal hyperplasia is generated. Moreover, the difference in mechanical property between a native artery and an artificial graft induces a hemodynamical flow disturbance and stress concentration near the anastomosed site, thereby enhancing thrombus formation and neointimal hyperplasia. Therefore, it is highly apparent that a small-diameter artificial graft essentially requires compliance matching with the native arteries as much as possible.

Compliant design

A few approaches to biomechanically adopted artificial grafts that respond to the periodic pulsatile stress to generate periodic distension have been experimentally developed. The main technological feature of this new "mechano-active" graft is the use of a durable synthetic elastomer, SPU, as a substrate, coupled with laser-ablated microporing with computer-assisted designing (CAD) and computer-assisted manufacturing (CAM) (16,17). A SPU tube was multiply micropored with the excimer laser (KrF: 248 nm) ablation to produce microporous thin-walled SPU tubes (wall thickness: 100 μm; round-shaped pore size: 100 μm in diameter; inner diameter: 1.5 mm; length: 2.0 cm) with various pore densities. The high pore-density tube produced compliance or stiffness similar to that of human coronaries within the physiological pressure range (18). A coating of a mixed solution of heparin, bFGF and/or vascular endothelial growth factor (VEGF) and photoreactive gelatin as a photocurable artificial ECM completely covered the luminal and outer surfaces as well as filling the pores (19,20). Upon implantation of such a graft in the rat's abdominal aorta, the implanted grafts pulsated in response to the pulsatile flow. Transanastomotic endothelialization from the anastomotic site proceeded in an early period of implantation, followed by transmural endothelialization through micropores, which spread through the entire luminal surface at a later period of implantation. Neither thrombus formation nor intimal hyperplasia were observed.

On the other hand, the significance of compliance matching as well as porosity on the patency of the grafts is a controversial issue and has been discussed over the years. The differentiated roles of compliance and porosity may provide us with an insight into the etiology of intimal hyperplasia. However, to address the question as to which effect, porosity or compliance, predominantly contributes to vessel patency, a well-designed experimental model was devised to eliminate other factors involved in intimal hyperplasia, such as antithrombogenic potential and foreign body reactions, both of which are caused by the graft materials, that confound in vivo studies. To clarify this important issue, the following three models, utilizing thin SPU tubes (wall thickness: 100 μm) with or without controlled micropores created by the excimer laser ablation technique, were designed and tested in vivo (21): Model I (microporous, permeable and compliant); Model II (controlled ablation creat-

ing deep grooves but leaving 5 μm of non-ablated layer in the wall; smooth-surfaced, impermeable and compliant); and Model III (non-ablated tubes; smooth-surfaced, impermeable and non-compliant). In Models I and II, the pore or groove size (diameter: 100 μm) and pore or groove arrangement were fixed, and consequently their compliances were almost identical. Irrespective of the model, the luminal surfaces were coated with benzophenone-derivatized gelatin and subsequently photocured. Twenty grafts (length: 20 mm) of each model were implanted in the abdominal aortas of rats for up to twenty-four weeks. The total patency rate decreased in the order of Model I > II > III grafts. All of the patent grafts were completely endothelialized after twelve weeks of implantation, irrespective of the model. Twenty-four weeks after implantation, in Model I grafts the neoarterial wall was thin, and smooth muscle cells (SMCs) were of the contractile phenotype. In Model II grafts the neoarterial wall exhibited considerable thickening. In Model III grafts the neoarterial wall exhibited marked thickening, and SMCs were of the synthetic phenotype. The neoarterial wall thickness in the midportion of the grafts after twenty-four weeks of implantation increased in the order of Model I << II << III grafts. Overall, the porous compliant graft was superior to the non-porous compliant graft. The worst one was the non-porous, non-compliant graft. Thus, the significance of the roles of porosity and compliance was differentiated. In addition, this study clearly demonstrated that compliance matching and porosity synergistically resulted in neoarterial wall restoration without appreciable thickening.

Recently, a new design concept based on a biomechanical design was proposed and fabricated, and prototype devices were tested in a canine model: a coaxial double-tubular compliant graft biomimicking the "J" curve of canine common carotid arteries using micropored SPU tubes (22,23). The coaxial double-tubular compliant graft was assembled by inserting the high-compliance inner tube into the low-compliance outer tube. By increasing the intraluminal hydrodynamic pressure, the inner tube inflates markedly in the low-pressure regions, and after the inner tube came into contact with the outer tube, both tubes inflated together gradually in the high-pressure regions. The wall thickness, pore diameter and density (relative area of micropores), which are the principal parameters determining the pressure-dependent diameter change, were adjusted according to the design criteria of the graft. This fabricated coaxial double-tubular graft exhibited the "J" curve mimicking that of target canine carotid arteries. Surface processing, which aimed to reduce thrombus formation on the luminal surface of the inner tube in the early stage of implantation and prevent tissue-mediated adhesion between the inner and outer tubes, and also between the outer tube and the surrounding tissues, was conducted by photochemical grafting of hydrophilic polymers. Upon implantation into the canine carotid arteries, the implanted grafts pulsated in response to the pulsatile flow, and the vascular morphogenesis proceeded with implantation duration. Tissue adhesion gradually occurred with implantation duration, resulting in a steeper "J" curve for a longer implantation period. A higher performance tissue-adhesion-preventing hydrophilic material is essentially required. Thus, the coaxial double-tubular graft was theoretically realized, but the shortcoming of the current technology mentioned above should be eliminated in the near future.

TISSUE-ENGINEERED VASCULAR GRAFT

Cell sourcing

The major issue in vascular tissue engineering is cell sourcing: how to harvest or recruit a sufficient amount of the vascular cell types, particularly ECs, which are natural non-thrombogenic luminal lining cells. To this end, a few approaches have been developed as follows.

Autologous vascular cells and collagen-based vascular grafts

Various types of collagen-based vascular tissues with autologous vascular cells harvested from veins have been devised and tested in vitro and in vivo. Utilizing the unique characteristics of spontaneous thermal gelation of type I collagen solution at physiological conditions and entrapped cell-driven self-contraction, cell-innoculated hybrid vascular tissues, including three-layered vascular tissues, were prepared (originally proposed and devised by Weinberg and Bell (24)).

Three vascular tissue models were prepared on the luminal surfaces of artificial grafts using three vascular cell types: EC-seeded intimal tissue which formed on collagen gel (Model I) (25), layer-by-layering of an EC-monolayered intimal layer and a SMC-innoculated medial layer (Model II) (26) and three-layered tissue structured hierarchically by an EC-monolayered intimal layer, a SMC-containing medial layer and a fibroblast-innoculated adventitial layer (Model III) (27). At up to one year of implantation, the canine models showed the following differentiated tissue morphogenesis potentials. Irrespective of the model, no thrombus was formed and

complete patency was obtained. This is primarily due to the natural non-thrombogenic potential of integrated monolayered ECs. However, the degree of tissue morphogenesis at cellular and ECM levels depended on the model type. Rapid subendothelial accumulation and circumferential orientation of SMCs (which was 100% synthetic type as seeded) was observed for Model III at three months after implantation, followed by Model II at six months after implantation. Concomitantly, phenotypic alteration from synthetic to contractile type of SMCs was observed in accordance with the progress of SMC accumulation and its cellular orientation. The highest degree of retardation of cellular events in medial tissue formation was observed in Model I, in which cellular migration, accumulation and orientation, and phenotypic alteration completed at approximately at twelve months after implantation. As for ECM regeneration, well-organized supramolecular ECM assemblies, such as the circumferential orientation of collagen bundles and the honeycomb-type structure of elastin, occurred in the order of Model III >> II >> I. Interestingly, although the thickness of the neoarterial tissue formed on the luminal surface of grafts increased as the implantation period proceeded from the early period of implantation, it tended to decrease with a further longer-term implantation period. This degeneration appeared to synchronously occur in a concerted manner of phenotypic alteration (redifferentiation) of SMCs, irrespective of the model type. Thus, it is concluded that a three-layered vascular tissue model possesses the vascular wall regeneration with the highest potential, followed by the bi-layer vascular tissue model.

When the mixture of three vascular cell types was embedded into a collagen gel, a time-dependent cell sorting-out or segregation occurred with implantation duration: the EC monolayer was at the top of the gel layer, followed by SMC accumulation and circumferential orientation, and fibroblasts existed at the outer layer (27). This spatio-cellulary-demanded remodeling may be derived from "nature's strategy".

This collagen gel-based technique was applied to fabricate "compliant" vascular grafts in which a cell-innoculated, cell-traction-driven dense tubular collagen gel was wrapped with a multiple-micropored elastomeric SPU sheet, which provided a "compliant" tissue-engineered vascular graft (28,29) that functioned well for canine implantation models. Preconditioning of the exposure of these engineered hybrid tissues by periodic circulation in an in vitro mock circuit prior to implantation promoted a higher degree of vascular tissue morphogenesis, including mechanical properties with higher pressure-resistant durability and larger mechanical strength, cellular orientation (31,32) and phenotypic alteration, and supramolecular organization (33) of structural biomacromoles including collagen and elastin.

On the other hand, when such a cell-innoculated tubular collagen gel was further cultured in vitro, an opaque elastomeric tubular hybrid vascular tissue without any scaffold was obtained. The breaking pressure of the hybrid tissue as the intraluminal pressure increased to approximately 100–130 mm Hg. Therefore, although such a hybrid tissue will not be able to withstand pulsatile stress in a high-pressure circulatory system, attempts have been made to use this hybrid tissue as a replacement for a diseased vein classified as a low-pressure circulatory system (34,35). Upon inplantation into veins after luminal endothelialization in a canine model, the patency was well maintained without rupture. The thrombus-free, monolayered ECs were noted. The wall thickness was dramatically increased from approximately 300 μm to 1200 μm in the early phase of implantation, but it was decreased to approximately 50 μm at six months after implantation, indicating that tissue-engineered veins appear to be mechanically adopted or remodeled in a low-pressure circulatory system. This process appeared to synchronously proceed as the degree of tissue architecture became high.

As an extension of a series of studies on hybrid vascular tissue, a branched hybrid graft was prepared using two different sizes of hybrid tissues that were assembled into a branched hybrid medial tissue by end-to-side anastomosis between two tubular hybrid medial tissues, and subsequently endothelialization occurred (36). The local hydrodynamic effect on lipid or protein uptake of fluorescent-labeled protein or lipid was determined by confocal laser scanning microscopy; the uptake was low at the high-shear zone in the branch region, while in the flow separation region the uptake was very high (37). These findings reflect region-specific tissue architecture in the branch region in response to the local flow pattern, and may provide an in vitro atherosclerosis model as well as lead to the development of functional branched hybrid grafts.

Tissue fragmentation

A series of Noishiki's pioneering works (38–42) on the seeding of fragmented tissues, such as autologous venous or adipose connective tissues, into commercially available artificial grafts markedly enhanced rapid tissue regeneration, including endothelialization. The principle of tissue fragmentation technology is to seed minced or fragmented tissues onto and into a highly porous fabric vascular prosthesis under